Bioorganic & Medicinal Chemistry 23 (2015) 7274–7281

Contents lists available at ScienceDirect

Bioorganic & Medicinal Chemistry

journal homepage: www.elsevier.com/locate/bmc

Fine tuning of agonistic/antagonistic activity for vitamin D receptor by 22-alkyl chain length of ligands: 22*S*-Hexyl compound unexpectedly restored agonistic activity

Yasuaki Anami [a], Yuta Sakamaki [a], Toshimasa Itoh [a], Yuka Inaba [a], Makoto Nakabayashi [b], Teikichi Ikura [c], Nobutoshi Ito [c], Keiko Yamamoto [a,*]

[a] *Laboratory of Drug Design and Medicinal Chemistry, Showa Pharmaceutical University, 3-3165 Higashi-Tamagawagakuen, Machida, Tokyo 194-8543, Japan*
[b] *School of Biomedical Science, Tokyo Medical and Dental University, Bunkyo-ku, Tokyo 113-8510, Japan*
[c] *Medical Research Institute, Tokyo Medical and Dental University, Bunkyo-ku, Tokyo 113-8510, Japan*

ARTICLE INFO

Article history:
Received 21 September 2015
Revised 18 October 2015
Accepted 19 October 2015
Available online 26 October 2015

Keywords:
Vitamin D
Nuclear receptor
X-ray crystallographic structure
Ligand-binding pocket
Partial agonist

ABSTRACT

1α,25-Dihydroxyvitamin D_3 exerts its actions by binding to vitamin D receptor (VDR). We are continuing the study related to the alteration of pocket structure of VDR by 22-alkyl substituent of ligands and the relationships between the alteration and agonistic/antagonistic activity. Previously we reported that compounds **2** (22-H), **3** (22*S*-Et), and **4** (22*S*-Bu) are VDR agonist, partial agonist and antagonist, respectively. Here, we describe the synthesis and biological evaluation of 22*S*-hexyl analog **5** (22*S*-Hex), which was designed to be a stronger VDR antagonist than **4**. Unexpectedly, **5** showed partial agonistic but not antagonistic activity when bound to VDR, indicating that it is not necessarily true that the bulkier the side chain is, the stronger the antagonistic activity will be. X-ray crystallographic analysis of the VDR–ligand-binding domain (VDR–LBD) accommodating compound **5** indicated that the partial agonist activity of **5** is dependent on the mixed population of the agonistic and antagonistic conformations. Binding of compound **5** may not bring the complex into the only antagonistic conformation due to the large conformational change of the VDR–LBD. From this study it was found that fine tuning of agonistic/antagonistic activity for VDR is possible by 22-alkyl chain length of ligands.

1. Introduction

1α,25-Dihydroxyvitamin D_3 (1α,25-$(OH)_2D_3$), **1**, is a hormone that plays a crucial role in the regulation of calcium homeostasis (Fig. 1). This hormone **1** is also known to be related to cell differentiation and proliferation and immunomodulation.[1] These physiological effects are initiated by the binding of the hormone to the vitamin D receptor (VDR). VDR is a member of nuclear receptors which act as ligand-dependent transcriptional factor.[2] VDR changes the conformation from inactive form to active form by ligand binding and then transcripts the target gene.[3]

As mentioned in our recent review,[4] vitamin D is now attracting attention because of its involvement in many acute and chronic illnesses related to calcium homeostasis, autoimmunity, cancer, diabetes, and cardiovascular and infectious diseases.[5–7] Accordingly, VDR ligands are expected as drugs to treat these diseases.[8,9] To develop such selective drugs, it is important to understand the structural basis of interactions between VDR and its ligand.

Several dozen crystal structures of the ligand binding domain (LBD) of VDR complexed with a ligand have been reported.[10] Most structures are the common active conformation of VDR–LBD and form a common pocket structure to accommodate the ligand.[11] Against such a background we are continuing the study related to the alteration of pocket structure by 22-alkyl substituent of the ligands and the relationships between the alteration and agonistic/antagonistic activity.[4,12–16] We previously reported that compounds **2** (22-H), **3** (22*S*-Et) and **4** (22*S*-Bu) are VDR agonist, partial agonist, and antagonist, respectively (Fig. 1).[13] Here, we report on the synthesis and biological evaluation of 22*S*-hexyl analog **5**, which was designed to be a stronger VDR antagonist than **4**. We also report on the X-ray crystallographic analysis of the VDR–LBD/**5** complex and VDR–LBD/**3** complex to understand the structural basis of their agonistic/antagonistic activities.

Abbreviations: VDR, vitamin D receptor; LBD, ligand-binding domain; 1α,25-$(OH)_2D_3$, 1α,25-dihydroxyvitamin D_3; SERM, selective estrogen receptor modulator; ERα, estrogen receptor α; PPARγ, peroxisome proliferator-activated receptor γ.

* Corresponding author. Tel./fax: +81 42 721 1580.
E-mail address: yamamoto@ac.shoyaku.ac.jp (K. Yamamoto).

http://dx.doi.org/10.1016/j.bmc.2015.10.026
0968-0896/

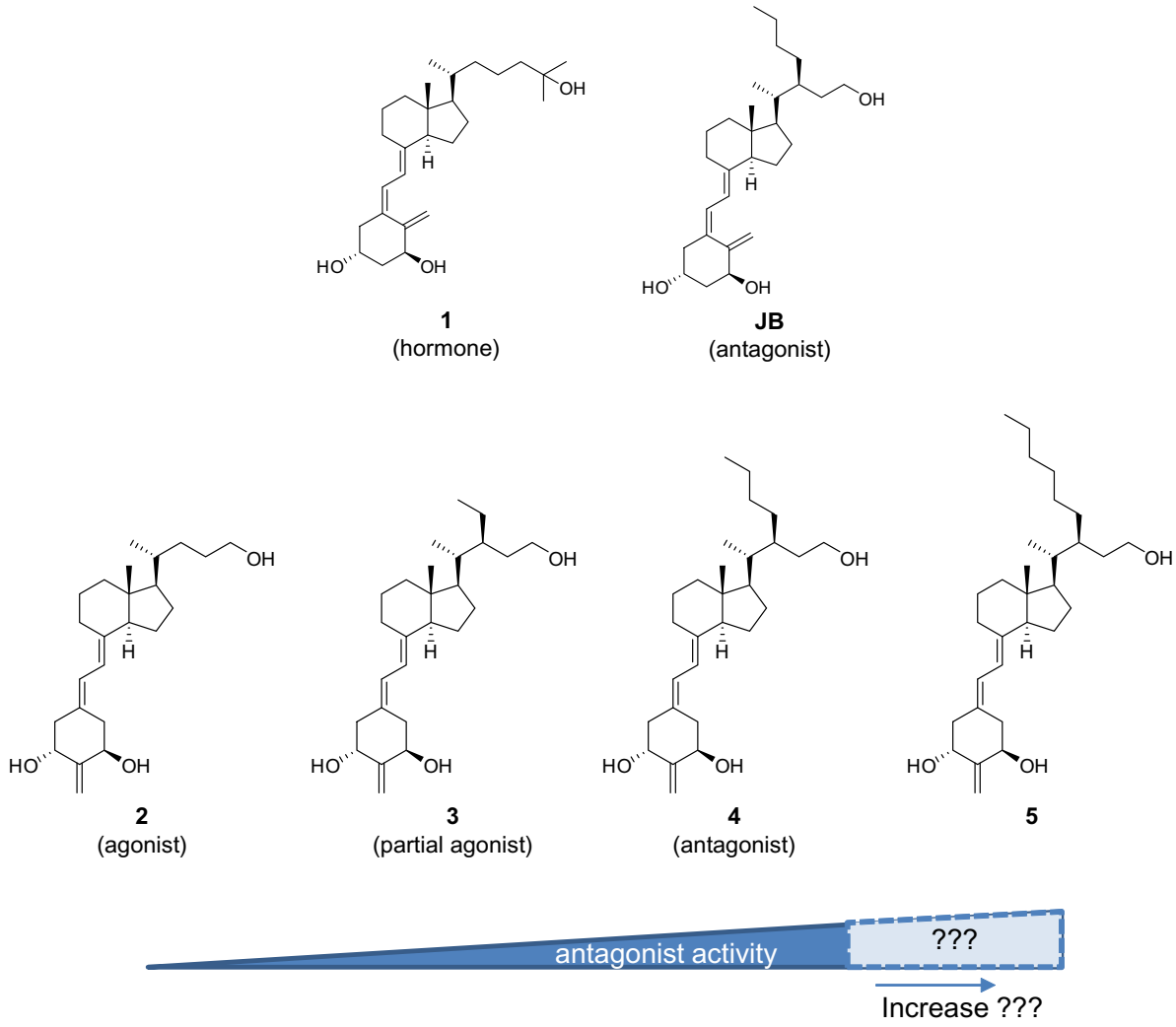

Figure 1. Structures of 1α,25-$(OH)_2D_3$ **1** and its analogs. Compounds **2** and **3** are agonist and partial agonist, respectively. **JB** and **4** are antagonist. Compound **5** was designed as a strong VDR antagonist.

2. Results

2.1. Synthesis

22*S*-Hexyl-24-hydroxy-19,25,26,27-tetranorvitamin D analog **5** was synthesized in a similar manner to that reported previously (Scheme 1).[13] Conjugate addition of Hex_2CuLi prepared from HexLi and $CuBr/Me_2S$ to *Z*-enoate **6** in the presence of TMSCl and HMPA proceeded diastereofacially to provide the 22*S*-isomer **7** in 62% yield and 22*R*-isomer **8** in 10% yield.[17] 22*S*-isomer **7** was reduced with DIBAL-H to give 24-alcohol **9** in 68% yield. Target compound **5** was obtained by deprotection of **9** with CSA in 85% yield.

2.2. Biological activities

Binding affinity for VDR was evaluated with a competitive binding assay using [^{3}H]-1α,25-dihydroxyvitamin D_3 (Fig. 2a). The IC_{50} values of **1** and **5** were 0.06 nM and 0.21 nM, respectively,

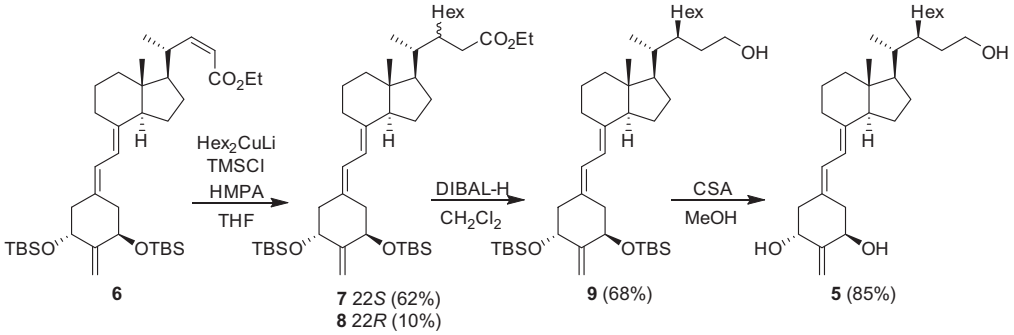

Scheme 1. Synthetic scheme of compound **5**.

indicating that 22*S*-hexyl compound **5** has approximately one-third the VDR affinity of compound **1**. Compared to compounds **2**–**4**, the strength order of binding affinity is **4** (22*S*-Bu) > **5** (22*S*-Hex) > **3** (22*S*-Et) > **2** (22-H).

The effect of compound **5** on transcriptional activity was evaluated using a luciferase reporter gene assay in Cos7 cells (Fig. 2b). Unexpectedly, compound **5** activated VDR and showed moderate agonistic activity. An inhibition assay using compound **5** was performed in the presence of 10^{-8} M of compound **1**. Compound **5** inhibited the activity of compound **1** in a concentration-dependent manner (Fig. 2c). These results indicate that compound **5** is not an antagonist but a partial agonist.

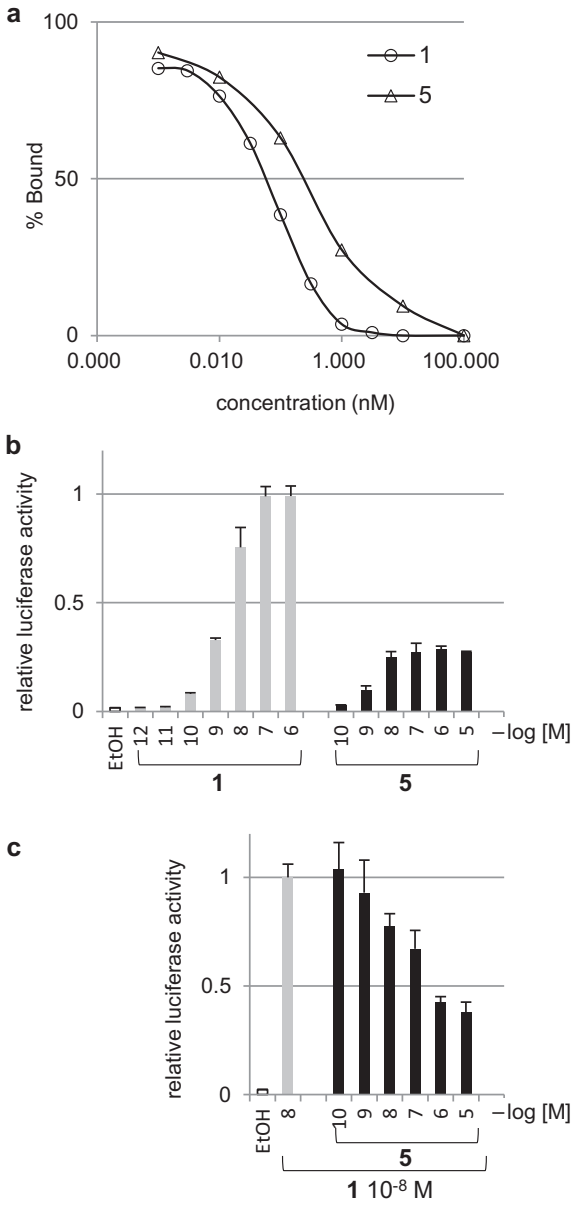

Figure 2. Binding affinity for VDR and transcriptional activity. (a) VDR binding affinity of compound **5**. The affinity was evaluated by competitive binding assay in duplicate. The IC_{50} values of **1** and **5** were determined by their concentration at 50% displacement of [^{3}H]-1α,25-$(OH)_2D_3$. (b and c) Effect of compound **5** on transcriptional activity in Cos7 cells. The transcriptional activity of **5** was evaluated at 10^{-10} to 10^{-5} M concentrations using dual luciferase assay in triplicate. (c) The inhibition effect on the transactivation induced by **1** was evaluated in the presence of 10^{-8} M of **1**.

2.3. X-ray crystal structure analysis

We previously reported the crystal structures of VDR–LBD complexed with agonist **2** (22-H) and antagonist **JB** (22*S*-Bu).[4,12,15] **JB** is recognized as a surrogate of antagonist **4** (22*S*-Bu). To clarify the molecular basis of the actions of 22*S*-alkyl compounds **3**–**5** relative to compound **1** and their prototype compound **2** (22-H), we carried out X-ray crystallographic analysis of VDR–LBD complexed with 22-Et compound **3** and 22-Hex compound **5**. X-ray diffraction images of complexes with **3** and **5** were obtained at 2.9 Å resolution and 2.2 Å resolution, respectively. Table 1 shows the data collection statistics and refinement. Both crystal structures had a space group of *C*2.

Figure 3a–c shows the crystal structure of VDR–LBD/**3** complex. The main chain structure of the protein is almost consistent with the canonical conformation (PDB 5AWK). The overall pocket structure is similar to VDR–LBD accommodating ligand **1** or **2**, but a slightly induced cavity in the direction of the butyl pocket was observed (Figs. 3a, 4b). The $2F_O - F_C$ map of ligand **3** is poor because of the low resolution (2.9 Å), but ligand **3** could be put into the map as shown in Figure 3b. The original side chain with the 24-hydroxyl group was accommodated into the canonical pocket and the 22*S*-ethyl group was directed to Leu305 (potential butyl pocket) (Fig. 3a). Interactions including hydrogen bonds between ligand **3** and VDR–LBD were similar to those of the VDR–LBD/**2** complex (Fig. 3c). One difference is the slight shift of the side chain of Leu305 caused by repulsion with the 22*S*-ethyl group (Figs. 3a, 4e).

Figure 3d–j shows the crystal structure of the VDR–LBD/**5** complex. The main chain structure of the protein adopted a canonical conformation (PDB 5AWJ). In this complex, a large butyl pocket and obvious side chain rotation of Leu305 were observed (Figs. 3d, 4e). Interestingly, composite omit map showed that ligand **5** binds to VDR–LBD with major and minor conformations in a ratio of approximately 6:4 (Fig. 3g–j) and whose side chains are inverted relative to one another. In the 60% major conformer, the original side chain with a 24-hydroxy group occupies the canonical pocket and the 22*S*-hexyl group occupies the butyl pocket as **JB** does

Table 1
Summary of data collection statistics and refinement

Ligand	**3**	**5**
X-ray source	KEK-PF BL-5A	SPring-8 BL38B1
Wavelength (Å)	1.00000	1.00000
Space group	*C*2	*C*2
Unit cell dimensions		
Bond (Å)	a = 154.03, b = 41.97, c = 41.86	a = 153.48, b = 44.45, c = 42.32
Angle (°)	α = 90.00, β = 95.96, γ = 90.00	α = 90.00, β = 100.53, γ = 90.00
Resolution range[a] (Å)	40.48–2.90 (3.10–2.90)	50.00–2.20 (2.28–2.20)
Total no. of reflections	9246	50,407
No. of unique reflections	4525	14,125
% completeness[a]	75.2 (76.8)	98.1 (85.7)
R_{merge}[a,b]	0.079 (0.309)	0.032 (0.138)
Refinement statistics		
Resolution range[a] (Å)	40.48–2.90 (3.10–2.90)	27.44–2.20 (2.28–2.20)
R factor (R_{free}/R_{work})[a,c]	0.2677/0.2094	0.2599/0.2139

[a] Values in parentheses are for the highest-resolution shell.

[b] $R_{merge} = \Sigma|(I_{hkl} - \langle I_{hkl}\rangle)|/(\Sigma I_{hkl})$, where $\langle I_{hkl}\rangle$ is the mean intensity of all reflections equivalent to reflection *hkl*.

[c] R_{work} (R_{free}) = $\Sigma||F_{obs}| - |F_{calc}||/\Sigma|F_{obs}|$, where 5% of randomly selected data were used for R_{free}.

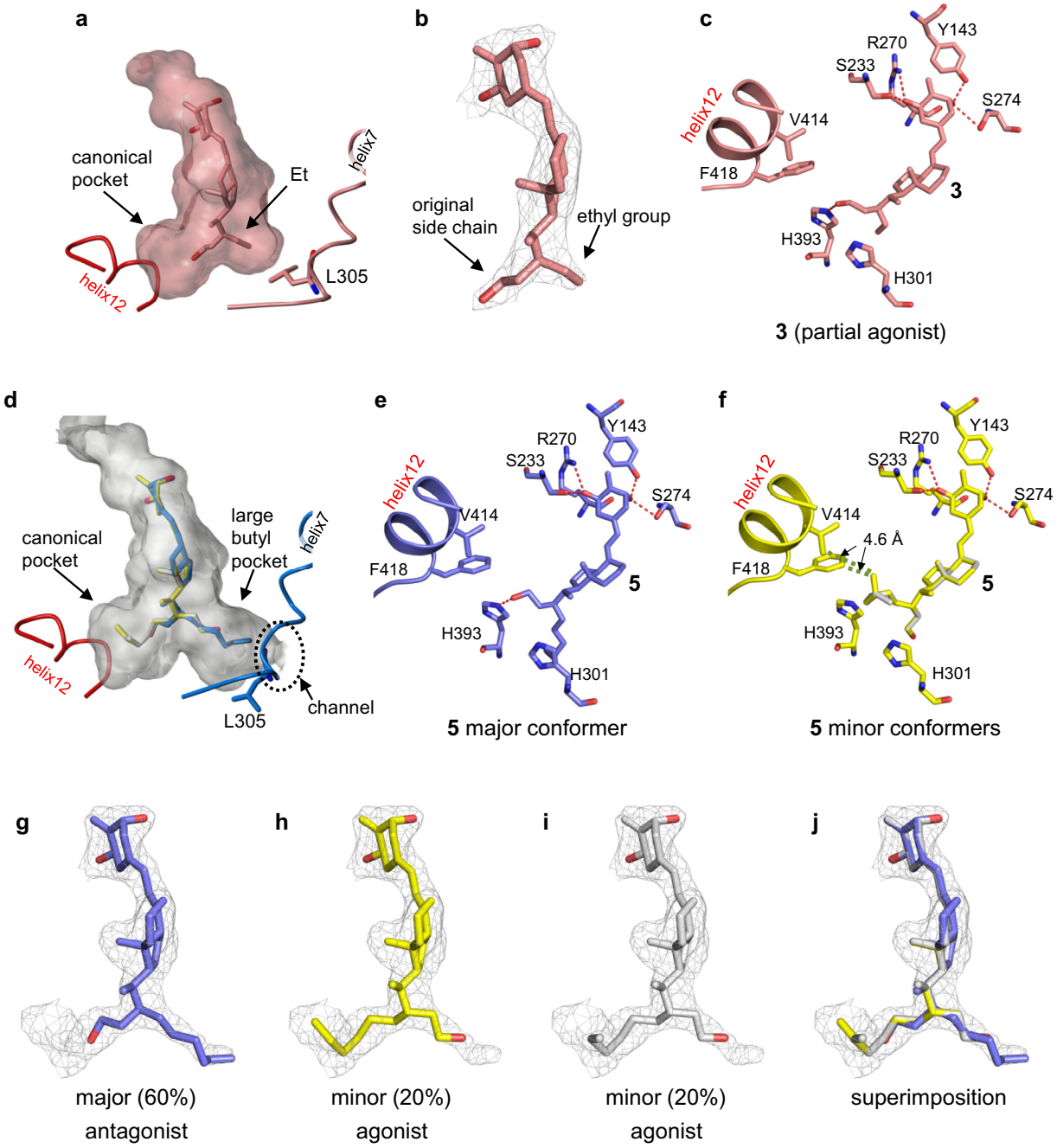

Figure 3. X-ray crystal structures of VDR–LBD complexed with **3** (a–c) and **5** (d–j). (a and d) Connolly channel surface of the ligand-binding pocket (LBP) of VDR–LBD/**3** (pink) and VDR–LBD/**5** (gray), which were calculated using software SYBYL-X 1.3. (b) The $2F_O - F_C$ map and the ligand **3** of VDR–LBD/**3** complex are shown as a gray mesh and pink stick, respectively. (g–j) The composite omit map of VDR–LBD/**5** complex was generated using the VDR–LBD without the ligand as a coordinate file and is shown as a gray mesh. There are three conformations of **5**, the major (blue stick) and the minor (yellow and gray sticks) conformers. (j) Superimposition of major and minor conformers of ligand **5**. (c, e and f) The hydrogen bonds between VDR–LBD and ligand, and the hydrophobic interactions between ligand and helix 12 (V414 and F418).

(Fig. 3d and g). In the 40% minor conformer, the original side chain occupied the butyl pocket and the 22*S*-hexyl group occupied the canonical pocket (Fig. 3d, h and i). The minor 40% conformer was further divided into a 20% conformer in which the terminal methyl of the 22*S*-hexyl group adopts different conformations (Fig. 3h and i). Superimposition of three conformers is consistent with the composite omit map (Fig. 3j). The large butyl pocket induced by compound **5** has a channel opening between helix 7 and helix 10 (Fig. 3d), which matches our previous observation.[16]

In all conformers, the 1α- and 3β-hydroxy groups of the A-ring formed pincer type hydrogen bonds with Ser233 and Arg270 and with Tyr143 and Ser274, respectively (Fig. 3e and f). In the major conformer, the 24-hydroxy group formed a hydrogen bond only with His393. Hydrophobic interactions with helix 12 were not observed (Fig. 3e). In the minor conformers, the 24-hydroxy group formed no hydrogen bond with any amino acid residues, while the terminal methyl of the hexyl group showed hydrophobic interactions with Val414 and Phe418 on helix 12 (Fig. 3f).

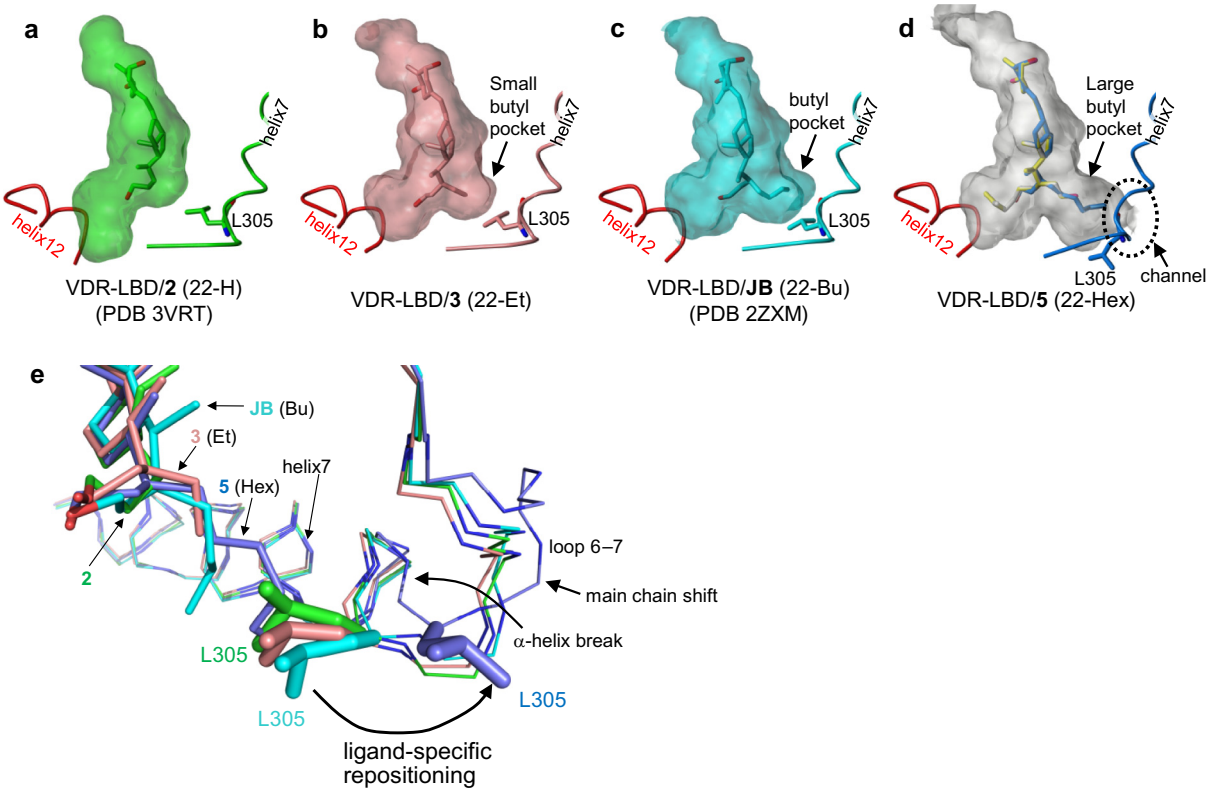

Figure 4. Connolly channel surface of the LBP of VDR–LBD/22*S*-alkyl compounds and structural alteration by rotation of Leu305. (a) The LBP of VDR–LBD/**2** (green, PDB 3VRT), which was depicted after generating Leu400 from the stub of the corresponding amino acid residue by examining the $2F_O - F_C$ map. (b) The LBP of VDR–LBD/**3** (pink), (c) VDR–LBD/**JB** (cyan, PDB 2ZXM), and (d) VDR–LBD/**5** (gray). (e) Superimposition of VDR–LBD/ligand complexes. Complexes of VDR–LBD with **2**, **3**, **JB**, and **5** are depicted in green, pink, cyan, and blue, respectively. The main chains (nitrogen of amide, α-carbon, and carbonyl carbon) are each shown as a slim stick, ligands are each shown as a stick, and the side chains of Leu305 are each shown as a thick stick. Leu305 of the VDR–LBD/**5** complex was drastically repositioned due to a steric repulsion with 22*S*-hexyl group, causing the main chain to move considerably.

3. Discussion

We have previously reported that compounds **2** (22-H), **3** (22*S*-Et) and **4** (22*S*-Bu) are VDR agonist, partial agonist and antagonist, respectively.[13] Here, we designed and synthesized a 22*S*-hexyl analog **5** as a stronger VDR antagonist than **4**, hypothesizing that a hexyl side chain bulkier than butyl would extend or break the butyl pocket, causing compound **5** to be a strong VDR antagonist. However, biological activities indicated that compound **5** is not an antagonist but a partial agonist. Specifically, compound **5** restored the agonist activity. The result suggested that an alkyl chain of appropriate length is needed for a ligand to act as an antagonist for VDR.

In crystals of the VDR–LBD/**5** complex, ligand **5** is accommodated into VDR–LBD with major and minor conformations (Fig. 3d–j). The binding mode of the major conformer was similar to that of antagonist **JB** in the following points: 22*S*-alkyl group occupying the butyl pocket, 24-hydroxyl group forming a hydrogen bond only with His393 but not His301, and the ligand not interacting hydrophobically with helix 12. As reported previously in our papers,[12,16] this conformation is thought to be temporary and less preferred but could be trapped during crystallization process by the effects of crystal packing, so this conformation seems to reflect antagonist binding structure. Therefore, the major conformer may be a conformation associated with an antagonistic activity, while minor conformers may be conformations associated with an agonistic activity. Recently we reported the crystal structure of VDR–LBD accommodating the partial agonist in which the ligand binds to VDR–LBD in two conformations, one of which is the antagonist/VDR–LBD complex structure and the other the agonist/VDR–LBD complex structure.[16] In that report, we concluded that partial agonist activity is dependent on the population of agonistic and antagonistic conformations. Similarly, in the present study, plural conformations were detected in a single crystal, so it is possible that the partial agonist activity of **5** depends on the mixed population of agonistic and antagonistic conformations. Thus, we could again trap conformational subsets of the ligand and the nuclear receptor in a single crystal.

Ligand **3** bound to VDR–LBD with a single conformation in a single crystal (Fig. 3a–c). Although an obvious butyl pocket was not induced, a small expanded cavity caused by repulsion with the ethyl group was observed. The $2F_O - F_C$ map of the ligand was not clear (Fig. 3b). From these results, in the case of partial agonist **3**, an inverted side chain conformer like compound **5** may exist in solution (living cells) although we cannot detect them in the crystals. Because the overall structure and binding mode of VDR–LBD/**3** complex were almost the same as those of the VDR–LBD/agonist **2** complex, the crystal structure observed here (Fig. 3a–c) would be the structure reflecting the agonist conformation but not the antagonist. The partial agonism of compound **3** may also be controlled by the population of agonistic and antagonistic conformations also seen in partial agonist **5**.

Figure 4 shows the pocket structures of VDR–LBD accommodating ligand **2** (22-H), **3** (22*S*-Et), **JB** (22*S*-Bu), and **5** (22*S*-Hex). In the previous paper,[16] we reported that there are two forms of the butyl pocket in which the first form is induced by the butyl group of the ligand and the second form is induced by a side chain bulkier than the butyl group. The first is formed by a small shift in the side chain of Leu305 (Fig. 4c and e), while the second is formed by a rotamer of the β-carbon of Leu305 (3WT5, 3WT6, 2HCD[18]). In the present

study, the latter butyl pocket was observed in the VDR–LBD/**5** complex (Fig. 4d), in which Leu305 exists as side chain rotamer and the α-helix break occurs at the beginning of helix 7 (Fig. 4e). Interestingly, we noticed in both the present and previous studies that the ligand-binding pocket having the second type of butyl pocket commonly accommodates multiple ligand conformers. Although the co-crystallization was barely achieved, VDR–LBD accommodating the hexyl group in the large butyl pocket (major conformer) may be unstable and consequently behave as an antagonist binding VDR; while VDR–LBD accommodating the hexyl group in the canonical pocket (minor conformer) may be stable and consequently behave as an agonist binding VDR. The minor conformer lacks hydrogen bonding with the side chain of the ligand but does show hydrophobic interactions with the hexyl groups, suggesting that the hydrophobic interactions may compensate for the disadvantage of no hydrogen bonding.

22*S*-Hexyl compound **5** was designed and synthesized as a potent VDR antagonist candidate but instead behaved as a partial agonist. Taken together, compounds **2** (22-H), **3** (22*S*-Et), **4** (22*S*-Bu) and **5** (22*S*-Hex) are VDR agonist, partial agonist, antagonist, and partial agonist, respectively. The present study indicates that it is not necessarily true that the bulkier the side chain is, the stronger the antagonistic activity will be. Consequently we found that fine tuning of agonist/antagonist activity for VDR is possible using a variety of 22-alkyl chain length of ligands.

Several mechanisms of partial agonistic action on nuclear receptors have been proposed (Fig. 5). First, partial agonist activity of selective estrogen receptor modulators (SERMs), raloxifene and tamoxifen, which exert their activity by binding to estrogen receptor α (ERα), is considered to be dependent on AF-1 domain but not helix 12 (AF2).[19–21] Helix 12 in crystal structures of the ERα-LBD/SERM complex localizes at the coactivator binding site, which is thought to be an antagonist binding structure, but SERMs show partial agonist activity because AF-1 domain retains transcriptional activity.

The second proposed mechanism is that partial agonist activity is exerted by a suboptimal conformation upon ligand binding. Pike et al. reported that helix 12 in the crystal structure of ERβ-LBD complexed with a partial agonist localizes at a position distinct from the agonistic position and is instead found in a similar orientation to the antagonistic position.[22] They considered that this conformation results in suboptimal positioning of helix 12. In peroxisome proliferator-activated receptor γ (PPARγ) and retinoid X receptor α, Oberfield et al., Bruning et al. and Ohsawa and Kawata et al. reported that partial agonists cannot adequately stabilize helix 12 compared to full agonists.[23–26]

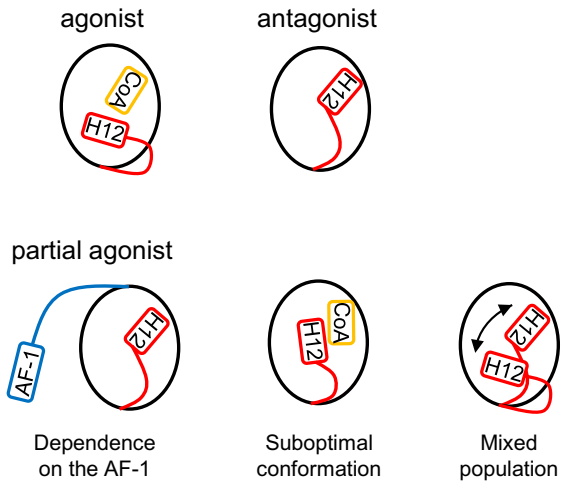

Figure 5. The conformation model of nuclear receptor by ligand binding. When agonist binds to the receptor, helix 12 (H12) is folded and the receptor recruits coactivator (CoA). When antagonist binds to the receptor, H12 localizes at the CoA binding site. There are three models that explain partial agonist activity. The first model is dependent on AF-1. The second model is based on a suboptimal conformation in which H12 exists in a different position from either the agonistic or antagonistic position. The third model is based on an average of the population of agonistic and antagonistic conformations.

The third proposed mechanism is that partial agonist activity is dependent on a population of agonistic and antagonistic conformations. We found that not only 22*R*-butyl analog[16] but also 22*S*-hexyl analog **5** bind to VDR–LBD with both agonistic and antagonistic conformations in a single crystal. Therefore, we conclude that partial agonistic activity of the 22*R*-butyl analog and the 22*S*-hexyl analog **5** is dependent on the sum of agonistic and antagonistic behaviors of the ligands on VDR. Nakabayashi et al. also reported a similar explanation for VDR partial agonism.[27] Bourguet et al. and Albers et al. reported that the equilibrium between the agonist position of helix 12 and its antagonist position in the coactivator binding groove may then depend on cellular context, and agonistic and antagonistic conformations depend on the interaction with cofactors (coactivators and corepressors) that help to stabilize either agonistic or antagonistic conformations, respectively.[28,29] Bruning et al. reported that agonistic and antagonistic conformations could both be detected in each different crystal structure by using wild type and mutated ERα-LBD.[30] Pochetti et al. also reported that the different binding mode of a partial agonist could be observed in separate crystals that were produced by a different procedure.[31] Recently we reported crystal structures of the complex of PPARγ-LBD and a partial agonist, in which two conformations, an active conformation and an alternative conformation, were observed.[32] All these results are consistent with the proposed mechanism that partial agonist activity is dependent on the equilibrium between agonistic and antagonistic conformations. That equilibrium may depend on the cellular context (e.g., the concentration of coactivators and corepressors), thus partial agonists may be potential candidates for pharmaceutical agents to treat various diseases.

4. Conclusion

We designed and synthesized 22*S*-hexyl analog **5** as a strong VDR antagonist but found that compound **5** acts as a partial agonist. The crystal structure of the VDR–LBD/**5** complex showed that ligand **5** binds to VDR with two conformations. Binding modes indicate that the major conformer is the structure associated with antagonistic activity, while minor conformers are structures associated with agonistic activity. Therefore the partial agonist activity observed with compound **5** may be explained by the mixed population of these agonistic and antagonistic conformations. In a series of 22*S*-alkyl compounds **2**–**5**, antagonist activity increases in the order of **2** (H) < **3** (Et) < **4** (Bu), but unexpectedly **5** (Hex) restores agonist activity. These results indicate that fine tuning of agonistic/antagonistic activity for VDR is possible by 22-alkyl chain length of ligands. This knowledge will be useful for the design of novel agonists/antagonists of VDR.

5. Experimental

5.1. General procedure

All reagents were purchased from commercial sources. NMR spectra were recorded with Bruker AV-300 M at 300 MHz for ^{1}H NMR and 75 MHz for ^{13}C NMR in $CDCl_3$ solution with TMS as an internal standard and the chemical shifts are given in δ values. High and low resolution mass spectra were obtained with a JEOL

JMS-HX110A and Shimadzu GCMS-QP5050A spectrometers. Relative intensities are given in parentheses in low mass. IR spectra were recorded on a Shimadzu FTIR-8400S spectrophotometer, and data are given in cm^{-1}. UV spectra were recorded on a Beckman DU7500 spectrophotometer. All air and moisture sensitive reactions were carried out under argon or nitrogen atmosphere. Purity was determined by HPLC [Pegasil silica SP100, 4.6 mm × 150 mm, hexane/$CHCl_3$/MeOH (100:25:8), flow rate 1.0 mL/min] and was >98.5% for tested compound.

5.2. Synthesis

5.2.1. Ethyl (3*S*)-3-{1-[(1*R*,3*R*,7*E*,17β)-1,3-bis{[*tert*-Butyl(dimethyl)silyl]oxy}-2-methylidene-9,10-secoestra-5,7-dien-17-yl]ethyl}nonanoate (7)

A suspension of CuBr/Me_2S (322 mg, 1.57 mmol) in THF (3 mL) was cooled to −25 °C, and to this solution was added hexyl lithium (1.35 mL, 3.12 mmol, 2.3 M in hexane) and the mixture was stirred for 20 min. To this solution was added TMSCl (249 μL, 1.95 mmol), HMPA (341 μL, 1.95 mmol), and a solution of *Z*-enoate **6** (83.4 mg, 0.13 mmol) in THF (2 mL) in this order. The mixture was stirred at −25 °C for 1.5 h, and the reaction was quenched with 3.6% HCl. The mixture was extracted with AcOEt. The organic layer was washed with water and brine, dried over $MgSO_4$ and evaporated. The residue was chromatographed on silica gel (10 g) with 0.5% AcOEt/hexane to afford **7** (58.4 mg, 62%) and its 22*R*-isomer **8** (12.6 mg, 10%).

7 ^{1}H NMR (300 MHz, $CDCl_3$) δ 0.02, 0.05, 0.07, 0.08 (each 3H, s, SiMe), 0.52 (3H, s, H-18), 0.81 (3H, d, J = 6.2 Hz, H-21), 0.86, 0.90 (each 9H, s, *t*-Bu), 1.25 (3H, t, J = 7.1 Hz, —COOEt), 2.82 (1H, m, H-9), 4.13 (2H, m, —COOEt), 4.43 (2H, m, H-1, 3), 4.92, 4.97 (each 1H, s, —C=CH_2), 5.84 (1H, d, J = 11.1 Hz, H-7), 6.21 (1H, d, J = 11.1 Hz, H-6). ^{13}C NMR (75 MHz, $CDCl_3$) δ −5.1, −4.91, −4.86 (2 carbons), 12.0, 13.2, 14.1, 14.4, 18.2, 18.3, 22.1, 22.7, 23.5, 25.78 (3 carbons), 25.85 (3 carbons), 27.3, 28.0, 28.1, 28.8, 29.7, 31.9, 37.4, 37.8, 38.5, 38.6, 40.7, 45.7, 47.6, 53.8, 56.3, 60.0, 71.6, 72.6, 106.3, 116.2, 122.4, 132.8, 141.1, 153.0, 173.9. MS (EI) *m*/*z* (%) 728 (M^+, 2), 596 (34), 539 (9), 366 (31), 234 (14), 147 (14), 73 (100). HRMS (EI) calcd for $C_{44}H_{80}O_4Si_2$ (M^+) 728.5595, found 728.5603. IR (neat) 3394, 2955, 2928, 2895, 2856, 1738, 1651 1620, 1464, 1256, 1101, 1070, 935, 897, 835, 775 cm^{-1}. UV (hexane) λ_{max} 246, 254, 264 nm.

8 (22*R*-isomer of **7**) ^{1}H NMR (300 MHz, $CDCl_3$) δ 0.03, 0.05, 0.07, 0.08 (each 3H, s, SiMe), 0.56 (3H, s, H-18), 0.79 (3H, d, J = 6.7 Hz, H-21), 0.87, 0.89 (each 9H, s, *t*-Bu), 2.82 (1H, m, H-9), 4.14 (2H, q, J = 7.2 Hz, —COOEt), 4.42 (2H, m, H-1, 3), 4.92, 4.97 (each 1H, s, —C=CH_2), 5.84 (1H, d, J = 11.0 Hz, H-7), 6.21 (1H, d, J = 11.2 Hz, H-6).

5.2.2. (3*S*)-3-{1-[(1*R*,3*R*,7*E*,17β)-1,3-bis{[*tert*-Butyl(dimethyl)silyl]oxy}-2-methylidene-9,10-secoestra-5,7-dien-17-yl]ethyl}nonan-1-ol (9)

Ester **7** (32.5 mg, 0.0446 mmol) in CH_2Cl_2 (1 mL) was treated with DIBAL-H (140 μL of 1.0 M toluene solution, 0.14 mmol) at 0 °C for 0.5 h. The reaction was quenched with Rochelle salt aq solution and extracted with CH_2Cl_2. The organic layer was washed with brine, dried over $MgSO_4$ and evaporated. The residue was chromatographed on silica gel (5 g) with 5% AcOEt/hexane to afford **9** (22.6 mg, 68%).

9 ^{1}H NMR (300 MHz, $CDCl_3$) δ 0.03, 0.05, 0.06, 0.08 (each 3H, s, SiMe), 0.54 (3H, s, H-18), 0.81 (3H, d, J = 6.2 Hz, H-21), 0.86, 0.90 (each 9H, s, *t*-Bu), 2.82 (1H, m, H-9), 3.65 (2H, m, H-24), 4.43 (2H, m, H-1, 3), 4.92, 4.97 (each 1H, s, —C=CH_2), 5.83 (1H, d, J = 11.2 Hz, H-7), 6.22 (1H, d, J = 11.1 Hz, H-6). ^{13}C NMR(75 MHz, $CDCl_3$) δ −5.1, −4.91, −4.86 (2 carbons), 12.0, 13.3, 14.1, 18.2, 18.3, 22.2, 22.7, 23.5, 25.78 (3 carbons), 25.85 (3 carbons), 27.8, 28.5, 28.7, 28.8, 29.9, 32.0, 35.3, 36.5, 38.0, 38.6, 40.7, 45.7, 47.6, 53.8, 56.3, 61.9, 71.6, 72.6, 106.3, 116.2, 122.4, 132.8, 141.1, 153.0.

5.2.3. 22*S*-Hexyl-2-methylidene-19,25,26,27-tetranor-1α,25-dihydroxyvitamin D_3 (5)

A solution of **9** (22.6 mg, 0.0305 mmol) and camphor sulfonic acid (22.3 mg, 0.096 mmol) in MeOH (1 mL) was stirred at room temperature for 2 h. Aqueous $NaHCO_3$ was added and the mixture was extracted with AcOEt. The organic layer was washed with brine, dried over $MgSO_4$ and evaporated. The residue was chromatographed on silica gel (5 g) with 70% AcOEt/hexane to afford **5** (11.9 mg, 85%).

5 ^{1}H NMR (300 MHz, $CDCl_3$) δ 0.55 (3H, s, H-18), 0.80 (3H, d, J = 6.4 Hz, H-21), 0.88 (3H, m, H-methyl of hexyl), 3.64 (2H, m, H-24), 4.47 (2H, m, H-1, 3), 5.09, 5.11 (each 1H, s, —C=CH_2), 5.88 (1H, d, J = 11.3 Hz, H-7), 6.35 (1H, d, J = 11.2 Hz, H-6). ^{13}C NMR (75 MHz, $CDCl_3$) δ 12.0, 13.3, 14.1, 22.2, 22.7, 23.5, 27.8, 28.5, 28.7, 29.0, 29.9, 32.0, 35.3, 36.5, 38.0, 38.2, 40.5, 45.8 (2 carbons), 53.8, 56.4, 61.9, 70.7, 71.8, 107.7, 115.3, 124.2, 130.5, 143.3, 152.0. MS (EI) *m*/*z* (%) 458 (M^+, 40), 315 (21), 297 (25), 287 (13), 269 (18), 251 (19), 169 (47), 161 (44), 135 (100). HRMS (EI) calcd for $C_{30}H_{50}O_3$ (M^+) 458.3760, found 458.3770. IR (neat) 3356, 2926, 2856, 1715, 1659, 1620, 1452, 1377, 1045, 756 cm^{-1}. UV (EtOH) λ_{max} 246, 254, 263 nm. Purity was determined by HPLC [Pegasil silica SP100, 4.6 mm × 150 mm, hexane/$CHCl_3$/MeOH (100:25:8), flow rate 1.0 mL/min] and was >98.5%.

5.3. Binding affinity

The binding affinity for VDR–LBD was evaluated according to the procedure reported previously.[13,33]

5.4. Transactivation

Transactivation in Cos7 cells was measured by dual luciferase assay according to the procedure reported previously.[13,33]

5.5. Crystallographic analysis

5.5.1. Protein expression and purification

Expression of rat VDR–LBD (residues 116–423, Δ165–211) and the following cell-lysis and centrifugation were done by the procedure reported previously.[15,16]

5.5.2. Crystallization of VDR–LBD/3

A mixture of rat VDR–LBD in buffer (10 mM Tris–HCl, pH 7.0, 2 mM NaN_3, 2 mM TCEP) and a ligand (5 equiv) was incubated at room temperature for 30 min. Then coactivator peptide (H_2-N—KNHPMLMNLLKDN—$CONH_2$) derived from DRIP205 including receptor interacting domain 2 in buffer (25 mM Tris–HCl, pH 8.0, 50 mM NaCl, 2 mM TCEP, 2 mM NaN_3) was added. The mixture of VDR–LBD/ligand/peptide was allowed to crystallize by the vapor diffusion method using a series of precipitant solutions containing 0.1 M MOPS-Na (pH 7.0), 0.075–0.2 M sodium formate, 12–22% (w/v) PEG4000, and 5% ethylene glycol. Droplets for crystallization were prepared by mixing 1 μL of complex solution and 1 μL of precipitant solution, and droplets were equilibrated against 300 μL of precipitant solution at 20 °C. The mixture was stored at 20 °C, and crystals appeared after a few days.

5.5.3. Crystallization of VDR–LBD/5

Purified rat VDR–LBD solution in buffer (10 mM Tris–HCl, pH 7.0, 0.02 % (w/v) NaN_3, 10 mM DTT) was concentrated to about 0.75 mg/mL by ultrafiltration. To an aliquot (400 μL) of the protein solution was added a ligand (10 equiv) and the solution was incubated overnight at 4 °C. The solution was further concentrated to

attain about 65 μL, and then coactivator peptide (H_2N—KNHPMLMNLLKDN—$CONH_2$) derived from DRIP205 including receptor interacting domain 2 in buffer (25 mM Tris–HCl, pH 8.0, 50 mM NaCl, 10 mM DTT, 0.02 % (w/v) NaN_3) was added. The mixture of VDR–LBD/ligand/peptide was allowed to crystallize by the vapor diffusion method using a series of precipitant solutions containing 0.1 M MOPS-Na (pH 7.0), 0.05–0.2 M sodium formate, 12–22% (w/v) PEG4000, and 5% ethylene glycol. Droplets for crystallization were prepared by mixing 2.8 μL of complex solution and 1.4 μL of precipitant solution, and droplets were equilibrated against 500 μL of precipitant solution at 20 °C. The mixture was stored at 20 °C, and crystals appeared after a few days.

5.5.4. X-ray crystallographic analysis

Prior to diffraction data collection, crystals were soaked in a cryoprotectant solution containing 0.1 M MOPS-Na (pH 7.0), 0.075–0.2 M sodium formate, 12–22% (w/v) PEG4000, and 18–22% ethylene glycol. Diffraction data sets of VDR–LBD/**3** complex and VDR–LBD/**5** complex were collected at 100 K in a stream of nitrogen gas at beamline BL-5A of KEK-PF (Tsukuba, Japan) and BL38B1 of Spring-8 (Sayou, Japan), respectively. Reflections were recorded with an oscillation range per image of 1.0°. Diffraction data were indexed, integrated, and scaled using the program iMOSFLM[34,35] or HKL2000.[36] The structures of ternary complex were solved by the procedure reported previously.[16] The composite omit map of the VDR–LBD/**5** complex (calculated in CNS ver.1.3[37,38]) was generated using VDR–LBD without the ligand as a coordinate file. The coordinate data for the structures were deposited in Protein Data Bank with accession numbers 5AWK (VDR–LBD/**3** complex), and 5AWJ (VDR–LBD/**5** complex).

Author contribution

Planned experiments: Y.A., Y.S., T.It, K.Y.
Performed experiments: Y.A., Y.S., T.It, Y.I., M.N., T.Ik., N.I.
Wrote paper: Y.A., Y.S., M.N., K.Y.

Acknowledgements

This work was partially supported by Platform for Drug Discovery, Informatics, and Structural Life Science from the Ministry of Education, Culture, Sports, Science, and Technology, Japan and by a Grant-in-Aid for Scientific Research (no. 26460155) from the Ministry of Education, Culture, Sports, Science, and Technology, Japan. We also thank the MEXT-Supported Program for the Strategic Research Foundation at Private Universities (2013-2017) and the Takeda Science Foundation, Japan, for financial support. Synchrotron-radiation experiments were performed at the Photon Factory (Proposal No. 2013G656) for the VDR–LBD/**3** complex and Spring-8 (Proposal No. 2008B1424) for the VDR–LBD/**5** complex, and we are grateful for the assistance provided by the beamline scientists at the Photon Factory and Spring-8.

Supplementary data

Supplementary data associated with this article can be found, in the online version, at http://dx.doi.org/10.1016/j.bmc.2015.10.026.

References and notes

1. Pike, J. W.; Meyer, M. B.; Bishop, K. A. *Rev. Endocr. Metab. Disord.* **2012**, *13*, 45.
2. Jurutka, P. W.; Whitfield, G. K.; Hsieh, J. C.; Thompson, P. D.; Haussler, C. A.; Haussler, M. R. *Rev. Endocr. Metab. Disord.* **2001**, *2*, 203.
3. Jones, G.; Strugnell, S. a.; DeLuca, H. F. *Physiol. Rev.* **1998**, *78*, 1193.
4. Yamamoto, K.; Anami, Y.; Itoh, T. *Curr. Top. Med. Chem.* **2014**, *14*, 2378.
5. Wacker, M.; Holiack, M. F. *Nutrients* **2013**, *5*, 111.
6. Holick, M. F. *Curr. Drug Targets* **2011**, *12*, 4.
7. Gröber, U.; Spitz, J.; Reichrath, J.; Kisters, K.; Holick, M. F. *Dermato-Endocrinology* **2013**, *5*, 331.
8. Nagpal, S.; Na, S.; Rathnachalam, R. *Endocr. Rev.* **2005**, *26*, 662.
9. Kubodera, N. *Heterocycles* **2010**, *80*, 83.
10. Molnár, F. *Front. Physiol.* **2014**, *5*, 1.
11. Rochel, N.; Wurtz, J. M.; Mitschler, A.; Klaholz, B.; Moras, D. *Mol. Cell* **2000**, *5*, 173.
12. Inaba, Y.; Yoshimoto, N.; Sakamaki, Y.; Nakabayashi, M.; Ikura, T.; Tamamura, H.; Ito, N.; Shimizu, M.; Yamamoto, K. *J. Med. Chem.* **2009**, *52*, 1438.
13. Sakamaki, Y.; Inaba, Y.; Yoshimoto, N.; Yamamoto, K. *J. Med. Chem.* **2010**, *53*, 5813.
14. Inaba, Y.; Nakabayashi, M.; Itoh, T.; Yoshimoto, N.; Ikura, T.; Ito, N.; Shimizu, M.; Yamamoto, K. *J. Steroid Biochem. Mol. Biol.* **2010**, *121*, 146.
15. Yoshimoto, N.; Sakamaki, Y.; Haeta, M.; Kato, A.; Inaba, Y.; Itoh, T.; Nakabayashi, M.; Ito, N.; Yamamoto, K. *J. Med. Chem.* **2012**, *55*, 4373.
16. Anami, Y.; Itoh, T.; Egawa, D.; Yoshimoto, N.; Yamamoto, K. *J. Med. Chem.* **2014**, *57*, 4351.
17. Yamamoto, K.; Ogura, H.; Jukuta, J.; Inoue, H.; Hamada, K.; Sugiyama, Y.; Yamada, S. *J. Org. Chem.* **1998**, *63*, 4449.
18. Ciesielski, F.; Rochel, N.; Moras, D. *J. Steroid Biochem. Mol. Biol.* **2007**, *103*, 235.
19. MacGregor, J. I.; Jordan, V. C. *Pharmacol. Rev.* **1998**, *50*, 151.
20. Berry, M.; Metzger, D.; Chambon, P. *EMBO J.* **1990**, *9*, 2811.
21. McInerney, E. M.; Katzenellenbogen, B. S. *J. Biol. Chem.* **1996**, *271*, 24172.
22. Pike, A. C.; Brzozowski, A. M.; Hubbard, R. E.; Bonn, T.; Thorsell, A. G.; Engström, O.; Ljunggren, J.; Gustafsson, J. A.; Carlquist, M. *EMBO J.* **1999**, *18*, 4608.
23. Oberfield, J. L.; Collins, J. L.; Holmes, C. P.; Goreham, D. M.; Cooper, J. P.; Cobb, J. E.; Lenhard, J. M.; Hull-Ryde, E. A.; Mohr, C. P.; Blanchard, S. G.; Parks, D. J.; Moore, L. B.; Lehmann, J. M.; Plunket, K.; Miller, A. B.; Milburn, M. V.; Kliewer, S. A.; Willson, T. M. *Proc. Natl. Acad. Sci. U.S.A.* **1999**, *96*, 6102.
24. Bruning, J. B.; Chalmers, M. J.; Prasad, S.; Busby, S. a.; Kamenecka, T. M.; He, Y.; Nettles, K. W.; Griffin, P. R. *Structure* **2007**, *15*, 1258.
25. Ohsawa, F.; Yamada, S.; Yakushiji, N.; Shinozaki, R.; Nakayama, M.; Kawata, K.; Hagaya, M.; Kobayashi, T.; Kohara, K.; Furusawa, Y.; Fujiwara, C.; Ohta, Y.; Makishima, M.; Naitou, H.; Tai, A.; Yoshikawa, Y.; Yasui, H.; Kakuta, H. *J. Med. Chem.* **2013**, *56*, 1865.
26. Kawata, K.; Morishita, K.; Nakayama, M.; Yamada, S.; Kobayashi, T.; Furusawa, Y.; Arimoto-Kobayashi, S.; Oohashi, T.; Makishima, M.; Naitou, H.; Ishitsubo, E.; Tokiwa, H.; Tai, A.; Kakuta, H. *J. Med. Chem.* **2015**, *58*, 912.
27. Nakabayashi, M.; Yamada, S.; Yoshimoto, N.; Tanaka, T.; Igarashi, M.; Ikura, T.; Ito, N.; Makishima, M.; Tokiwa, H.; DeLuca, H. F.; Shimizu, M. *J. Med. Chem.* **2008**, *51*, 5320.
28. Bourguet, W.; Vivat, V.; Wurtz, J. M.; Chambon, P.; Gronemeyer, H.; Moras, D. *Mol. Cell* **2000**, *5*, 289.
29. Albers, M.; Blume, B.; Schlueter, T.; Wright, M. B.; Kober, I.; Kremoser, C.; Deuschle, U.; Koegl, M. *J. Biol. Chem.* **2006**, *281*, 4920.
30. Bruning, J. B.; Parent, A. A.; Gil, G.; Zhao, M.; Nowak, J.; Pace, M. C.; Smith, C. L.; Afonine, P. V.; Adams, P. D.; Katzenellenbogen, J. A.; Nettles, K. W. *Nat. Chem. Biol.* **2010**, *6*, 837.
31. Pochetti, G.; Godio, C.; Mitro, N.; Caruso, D.; Galmozzi, A.; Scurati, S.; Loiodice, F.; Fracchiolla, G.; Tortorella, P.; Laghezza, A.; Lavecchia, A.; Novellino, E.; Mazza, F.; Crestani, M. *J. Biol. Chem.* **2007**, *282*, 17314.
32. Egawa, D.; Itoh, T.; Yamamoto, K. *Bioconjug. Chem.* **2015**, *26*, 690.
33. Inaba, Y.; Yamamoto, K.; Yoshimoto, N.; Matsunawa, M.; Uno, S.; Yamada, S.; Makishima, M. *Mol. Pharmacol.* **2007**, *71*, 1298.
34. Battye, T. G. G.; Kontogiannis, L.; Johnson, O.; Powell, H. R.; Leslie, A. G. W. *Acta Crystallogr., D: Biol. Crystallogr.* **2011**, *67*, 271.
35. Leslie, A. G. W.; Powell, H. R. Processing Diffraction Data with Mosflm. In *Evolving Methods for Macromolecular Crystallography*; Read, R. J., Sussman, J. L., Eds.; NATO Science Series II: Mathematics, Physics and Chemistry; Springer: Netherlands: Dordrecht, 2007; Vol. 245, pp 41–51.
36. Otwinowski, Z.; Minor, W. *Methods Enzymol.* **1997**, *276*, 307.
37. Brünger, A. T.; Adams, P. D.; Clore, G. M.; DeLano, W. L.; Gros, P.; Grosse-Kunstleve, R. W.; Jiang, J. S.; Kuszewski, J.; Nilges, M.; Pannu, N. S.; Read, R. J.; Rice, L. M.; Simonson, T.; Warren, G. L. *Acta Crystallogr., D: Biol. Crystallogr.* **1998**, *54*, 905.
38. Brunger, A. T. *Nat. Protoc.* **2007**, *2*, 2728.